frontiers in Marine Science

ORIGINAL RESEARCH
published: 13 September 2019
doi: 10.3389/fmars.2019.00563

DSi as a Tracer for Submarine Groundwater Discharge

Till Oehler[1]*, Joseph Tamborski[2], Shaily Rahman[3], Nils Moosdorf[1,4], Janis Ahrens[5], Corinna Mori[5], René Neuholz[5], Bernhard Schnetger[5] and Melanie Beck[5]

[1] Department Biogeochemistry and Geology, Leibniz Centre for Tropical Marine Research (ZMT), Bremen, Germany, [2] Department of Marine Chemistry and Geochemistry, Woods Hole Oceanographic Institution, Woods Hole, MA, United States, [3] Department of Geological Sciences, University of Florida, Gainesville, FL, United States, [4] Institute of Geosciences, Kiel University (CAU), Kiel, Germany, [5] Institute for Chemistry and Biology of the Marine Environment (ICBM), Carl von Ossietzky University of Oldenburg, Oldenburg, Germany

Submarine groundwater discharge (SGD) is an important source of nutrients and metals to the coastal ocean, affects coastal ecosystems, and is gaining recognition as a relevant water resource. SGD is usually quantified using geochemical tracers such as radon or radium. However, a few studies have also used dissolved silicon (DSi) as a tracer for SGD, as DSi is usually enriched in groundwater when compared to surface waters. In this study, we discuss the potential of DSi as a tracer in SGD studies based on a literature review and two case studies from contrasting environments. In the first case study, DSi is used to calculate SGD fluxes in a tropical volcanic-carbonate karstic region (southern Java, Indonesia), where SGD is dominated by terrestrial groundwater discharge. The second case study discusses DSi as a tracer for marine SGD (i.e., recirculated seawater) in the tidal flat area of Spiekeroog (southern North Sea), where SGD is dominantly driven by tidal pumping through beach sands. Our results indicate that DSi is a useful tracer for SGD in various lithologies (e.g., karstic, volcanic, complex) to quantify terrestrial and marine SGD fluxes. DSi can also be used to trace groundwater transport processes in the sediment and the coastal aquifer. Care has to be taken that all sources and sinks of DSi are known and can be quantified or neglected. One major limitation is that DSi is used by siliceous phytoplankton and therefore limits its applicability to times of the year when primary production of siliceous phytoplankton is low. In general, DSi is a powerful tracer for SGD in many environments. We recommend that DSi should be used to complement other conventionally used tracers, such as radon or radium, to help account for their own shortcomings.

Keywords: submarine groundwater discharge, DSi, silica, tracer, radon, radium

Edited by:
Ryo Sugimoto,
Fukui Prefectural University, Japan

Reviewed by:
Shiho Kobayashi,
Kyoto University, Japan
Yaser Nikpeyman,
Shahid Beheshti University, Iran

***Correspondence:**
Till Oehler
Till.Oehler@leibniz-zmt.de

Specialty section:
This article was submitted to
Marine Ecosystem Ecology,
a section of the journal
Frontiers in Marine Science

Received: *30 April 2019*
Accepted: *27 August 2019*
Published: *13 September 2019*

Citation:
Oehler T, Tamborski J, Rahman S, Moosdorf N, Ahrens J, Mori C, Neuholz R, Schnetger B and Beck M (2019) DSi as a Tracer for Submarine Groundwater Discharge. Front. Mar. Sci. 6:563. doi: 10.3389/fmars.2019.00563

INTRODUCTION

Submarine groundwater discharge (SGD) is an important source of nutrients and metals for the coastal ocean (Slomp and Van Cappellen, 2004; Moore, 2010), affects coastal ecosystems (Lecher and Mackey, 2018) and is a relevant and important water resource for coastal communities (Moosdorf and Oehler, 2017). SGD represents the discharge of terrestrial (fresh), marine (saline), or a mixture of both (brackish) groundwater (or pore water) into the ocean (Burnett et al., 2003; Moore, 2010).

Geochemical tracers have widely been applied to calculate SGD fluxes. This requires detailed knowledge of the tracer concentration coupled to potential sources and sinks, its residence time in the coastal water column and its endmember concentration in groundwater. Radium (Ra) and Radon (^{222}Rn) isotopes are commonly used as geochemical tracers for SGD, as both tracers are in general enriched in groundwater by several orders of magnitude compared to surface waters (Swarzenski, 2007; Moore, 2010). The "radium quartet" is advantageous for SGD quantification, as the wide range in half-lives of the four isotopes (^{223}Ra = 11.4 days, ^{224}Ra = 3.66 days, ^{226}Ra = 1,600 years and ^{228}Ra = 5.75 years) can be used to trace flow paths and processes over variable time-scales. However, Ra data should be interpreted cautiously when fluid ionic strength changes, which affects the partitioning of Ra between solid and solution phases (Webster et al., 1995; Beck and Cochran, 2013). Furthermore, Ra analyses typically require large sampling volumes (tens to hundreds of liters) (Moore and Reid, 1973) and rapid measurement after sampling, as the short-lived Ra isotopes decay within days to weeks. Radon (^{222}Rn = 3.83 days) is an inert noble gas that is not partitioned between solid and solution phases like its counterpart Ra. ^{222}Rn measurements are automated (Burnett and Dulaiova, 2003), which facilitates rapid data collection over large spatial areas (Dulaiova et al., 2010) and at stationary time-series. However, ^{222}Rn cannot be accurately applied as a tracer in high energy environments (winds, waves), as it is prone to degassing (Fanning et al., 1982).

Dissolved silicon (DSi) is also used as a geochemical tracer for SGD (Street et al., 2008; Garcia-Solsona et al., 2010a; Hernández-Terrones et al., 2011; Hwang et al., 2016; Lubarsky et al., 2018), but has received less attention than ^{222}Rn and Ra isotopes. DSi in groundwater is the product of chemical weathering of rocks and sediments, or dissolution of biogenic opal. Consequently, terrestrial and marine groundwater (or pore water) is often enriched in DSi (Rad et al., 2007; Anschutz et al., 2009) and can further be augmented during the passage through the subterranean estuary (STE) (Moore, 2010; Rahman et al., 2019). Consequently, SGD [including pore water exchange (PEX)] usually contains high DSi concentrations, which qualifies DSi as a useful addition to conventionally used tracers such as ^{222}Rn or Ra (Kim et al., 2005, 2008; Street et al., 2008; Garcia-Solsona et al., 2010b; Hwang et al., 2016; Tamborski et al., 2018). The advantages of DSi as a tracer for SGD include small sampling volumes, low detection limits and high precision measurements. Samples for DSi are easy to store and transport, which makes DSi logistically desirable as a tracer in remote areas with limited infrastructure, where it may be challenging to sample for ^{222}Rn and Ra isotopes. Furthermore, DSi is not prone to degassing, and may thus be a useful tool to compliment ^{222}Rn mass balances in high-energy environments. However, DSi does not behave conservatively in many coastal environments, where it can adsorb onto Fe-oxides or reprecipitates as amorphous Al-Si phases (e.g., Mackin and Aller, 1984). One of the main limitations of DSi as a tracer is that it is used by siliceous plankton (e.g., diatoms, flaggelates, radiolarians and picocyanobacteria) as well as higher trophical levels such as sponges, as a nutrient to build up their hard tissues (Brzezinski, 1985; Krause et al., 2011, 2017; Tréguer and De La Rocha, 2013). The aim of this study is to assess under which conditions DSi can be used as a tracer for SGD. We review the current state of the literature and show two case studies in contrasting geological environments to demonstrate the utility of DSi as a tracer for SGD.

DSi IN GROUNDWATER AND SURFACE WATER

DSi in Groundwater and the Subterranean Estuary

The concentration of DSi in fresh, brackish and marine groundwater is chiefly governed by dissolution rates of minerals in the aquifer and in the sediment (i.e., weathering; **Figure 1**, f) which is usually dependent on the lithology, the subsurface residence time of groundwater and biogeochemical transformations (Bluth and Kump, 1994; Horton et al., 1999; Jacobson et al., 2003; Rahman et al., 2019). Combined, these factors control DSi endmember concentrations in SGD. Indeed, different SGD flow paths (Santos et al., 2012) may lead to unique DSi endmember concentrations. For example, terrestrial groundwater (**Figure 1**, a) can have a different DSi endmember concentration compared to tidally driven marine groundwater (**Figure 1**, b). In either case, differences in DSi concentrations can be attributed to the above mentioned conditions, which are discussed in detail below.

In marine groundwaters, DSi concentrations are dominantly controlled by the dissolution of biogenic silica (e.g., DeMaster, 2002). Based on the dissolution of biogenic silica pore water DSi concentrations can reach 1000–1200 μM under typical pressure and temperature conditions found in marine sediments (e.g., Hurd, 1973; Schink et al., 1975; DeMaster, 2003; Loucaides et al., 2012). Alteration processes like incorporation of Al, adsorption of metals (e.g., Al^{3+} and Fe^{3+}) onto the silica substrate surface, formation of metal oxide coatings, or aging of the substrate inhibit the dissolution of biogenic opal (Van Cappellen and Qiu, 1997; Dixit and Van Cappellen, 2002; Van Cappellen et al., 2002; Michalopoulos and Aller, 2004; Khalil et al., 2007; Loucaides et al., 2010).

In most terrestrial groundwaters, the net silica enrichment is primarily controlled by lithogenic mineral dissolution (e.g., Ehlert et al., 2016), and thus depends on the lithology of the aquifer under study (**Table 1**; Rahman et al., 2019). Silicate mineral dissolution rates vary with pH, temperature, salinity, groundwater flow rates and sediment-water volume ratios (Oelkers and Gislason, 2001; Anschutz et al., 2009; Jeandel and Oelkers, 2015; Morin et al., 2015). Si saturation will be controlled by the type of Si-bearing minerals present. Thus, the maximum attainable DSi concentration in groundwater is a function of the surrounding environment. For example, karstic terrestrial groundwater has relatively low DSi concentration (80 ± 63 μM), reflecting the low Si

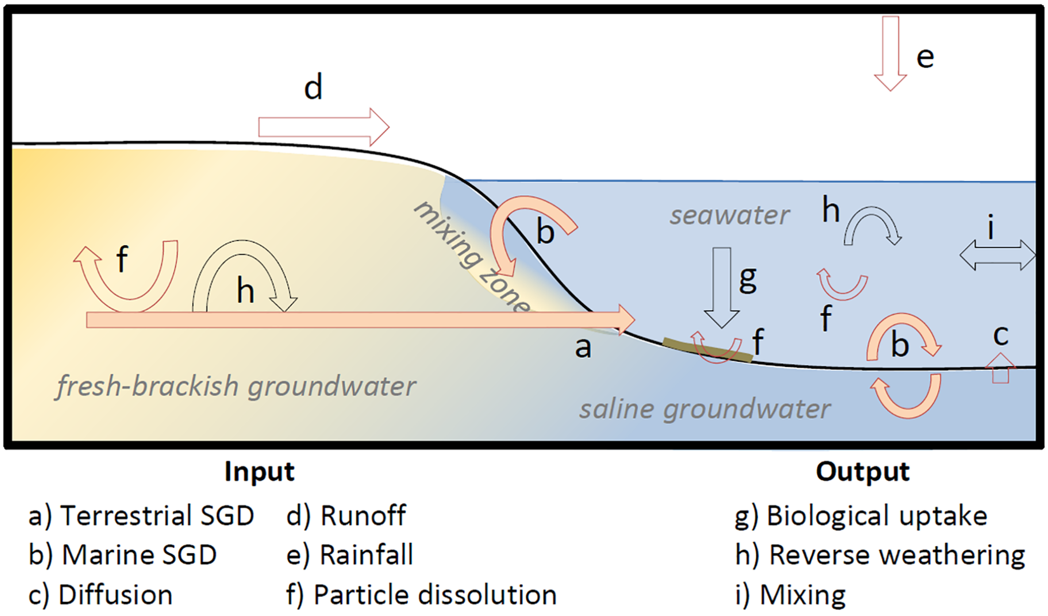

FIGURE 1 | Conceptual figure illustrating different processes governing DSi concentrations in coastal waters and coastal sediments/aquifer. Red arrows represent sources of DSi and black arrows represent sinks of DSi. Orange filled arrows represent hypothetical SGD flow paths, including terrestrial groundwater (a) and marine groundwater (b). Yellow colors represent fresh-brackish waters and blue colors represent saline water. The mixing zone between fresh and saline groundwater is called subterranean estuary (STE). The green line at the seafloor represents biogenic silica which has deposited e.g., after a phytoplankton bloom (Kowalski et al., 2013). The respective processes which lead to an input or output of DSi are labeled in the lower panel. Sources and sinks can vary with respect to the environmental boundary conditions, the size of the arrows is thus not representative for the quantity of their respective fluxes.

content of carbonates, whereas extrusive igneous groundwater is extremely enriched in DSi (604 ± 192 μM) (**Table 1**; Rahman et al., 2019).

Further, DSi concentration in groundwater can be modified during passage though the STE. Non-conservative behavior of DSi in groundwater may be assessed from the observed enrichment or deficit of DSi with respect to two-endmember linear mixing between fresh groundwater and surface marine waters. Whereas carbonate aquifers appear to show no net enrichment of DSi in brackish groundwaters, marine SGD flow paths from extrusive igneous and complex lithologies exhibit average net DSi enrichments of ∼50 μM globally (**Table 1**; Rahman et al., 2019, and references therein). Though there is evidence of non-conservative DSi behavior in aquifers composed of primarily granite (Onodera et al., 2007; Rengarajan and Sarma, 2015; Wang et al., 2015; Lecher et al., 2016), shale (Kim et al., 2005; Lee et al., 2012; Luo et al., 2014; Ye et al., 2016) and sandstone (Weinstein et al., 2011; Sugimoto et al., 2017) lithologies, the data are yet insufficient to constrain net DSi concentrations in marine SGD in these endmember lithologies globally (**Table 1**). At the land-sea transition, dissolution rates of terrestrially derived silicate-bearing mineral phases or silica substrates (e.g., phytoliths) are on average 4–5 times higher in seawater than in freshwater (Loucaides et al., 2008). These findings are consistent with other laboratory studies of basaltic glass or lithogenic particle dissolution in brackish waters (Daux et al., 1997; Advocat et al., 1998; Techer et al., 2001; Jones et al., 2012; Oelkers et al., 2012; Morin et al., 2015), as well as static and flow-through incubations of sediment at the freshwater-seawater transition zone in the STE (Anschutz et al., 2009; Ehlert et al., 2016; Tamborski et al., 2018). Dissolution rates of sediments of different lithologies, at solid surface to volume ratios close to those found in the STE, range from ∼3.4 to 49 mol Si m^{-2} s^{-1} (Techer et al., 2001; Anschutz et al., 2009; Ehlert et al., 2016; Tamborski et al., 2018).

TABLE 1 | Globally-averaged terrestrial and marine SGD DSi endmember concentrations categorized after lithology, summarized from Rahman et al. (2019).

	Terrestrial SGD DSi [μM]	Marine SGD DSi [μM]
Extrusive Igneous	604 ± 192	56 ± 43
Carbonate	80 ± 63	0
Sandstone	159 ± 80	
Granite	334 ± 255	
Shale	182 ± 91	
Complex lithology	288 ± 245	50 ± 41

Complex lithology is defined as more than one type of major lithology and includes unconsolidated glacial sediments.

The subsurface residence time of groundwater is directly proportional to the flow velocity and flow path length (i.e., transit time) and is thus tied to DSi enrichments via mineral dissolution kinetics. The longer a parcel of fluid is in contact with Si-bearing minerals, the greater DSi that fluid may obtain from water-rock weathering reactions, until a steady-state or transient steady-state is reached between Si dissolution and reprecipitation (Ehlert et al., 2016). In DSi-poor groundwaters, initial dissolution rates are high before Si concentrations stabilize. With longer pore fluid residence times and higher DSi concentrations, dissolution rates decrease (Techer et al., 2001). Coatings or secondary mineral phases form on the substrate, reducing the reactive surface area (Daux et al., 1997; Gislason and Oelkers, 2003). Higher flow velocities can increase dissolution rates as products of the dissolution reaction (i.e., dissolved Si or silicic acid) are transported away from their site of production and the reactions stay far from equilibrium (Anschutz et al., 2009). Due to continuous DSi enrichment in the pore fluid, some portion of the initially released DSi (30 to 60%) will reprecipitate into a secondary mineral phase (e.g., amorphous alumino-silicates), which is dependent on groundwater residence times (Daux et al., 1997; Staudigel et al., 1998). Terrestrial groundwater residence times can vary from days to thousands of years; similarly, marine groundwater residence times can vary from seconds to centuries (Seidel et al., 2015). Knowledge on the time-scale of the flow path under consideration is thus extremely important to evaluate DSi endmember concentrations.

DSi as an Indicator for Groundwater Transport Processes

Dissolved silicon may be used to quantify groundwater residence times when the factors described in section "DSi in Groundwater and the Subterranean Estuary" are considered. Anschutz et al. (2009) investigated the residence time of beach groundwaters based on the kinetics of quartz dissolution in seawater. Intertidal beach sand was incubated with seawater to determine the change in DSi concentration over time. Experiments can be performed under varying conditions, including seawater: sediment ratios, temperature and pH. In addition, incubations can be performed under "static" conditions or with seawater actively circulating with specified flow rates through the sediment. The dissolution rate of silicate minerals can be simply estimated from the linear increase in DSi concentration over time. This methodology has been successfully applied to several sediment types (Anschutz et al., 2009; Charbonnier et al., 2013; Ehlert et al., 2016; Tamborski et al., 2018). Groundwater residence times can be estimated for marine groundwater by assuming that there is no DSi contribution from terrestrial groundwater or from the dissolution of biogenic silica (Ehlert et al., 2016).

Dissolved silicon can also be used to determine if groundwater infiltration or exfiltration occurs within sediments. If the DSi concentration at two distinct depth horizons is known (e.g., 50 and 100 cm), the concentration gradient between both depths can delineate the advective transport of groundwater, assuming that biogeochemical transformations of DSi are negligible between both horizons. The underlying assumption is that in infiltration (recharge) zones, a positive gradient would indicate increasing release of the constituent (DSi) with increasing depth, while in exfiltration (discharge) zones a negative gradient would indicate increasing accumulation of the constituent (DSi) with decreasing depth. With this method, it was possible to visualize in- and exfiltration patterns in the intertidal zone of the beach system on Spiekeroog Island, southern North Sea (Waska et al., 2019).

DSi as a Tracer for SGD in Coastal Waters

If dissolved silicon is used as a tracer for SGD, several processes which affect DSi concentrations have to be considered (**Figure 1**). Inputs can occur from river and surface runoff (F_{runoff}) (**Figure 1**, d), rainfall (F_{rain}) (**Figure 1**, e), dissolution of particles in the water column and surface sediments ($F_{\text{dissolution}}$) (**Figure 1**, f), diffusion (F_{diff}) (**Figure 1**, c), and SGD (F_{SGD}) (**Figure 1**, a,b). Output terms include mixing with offshore waters (F_{mix}) (**Figure 1**, i), biological uptake (F_{biol}) (**Figure 1**, g), for example by benthic and pelagic siliceous plankton, and reverse weathering (F_{rev}) (**Figure 1**, h). Assuming steady-state conditions, and that DSi inputs equal DSi outputs, a simple DSi mass balance can be written (Eq. 1).

$$F_{\text{SGD}} + F_{\text{diff}} + F_{\text{runoff}} + F_{\text{rain}} + F_{\text{dissolution}} = F_{\text{mix}} + F_{\text{rev}} + F_{\text{biol}} \quad (1)$$

In coastal environments many of these processes are often time dependent. Over short time-scales (e.g., tidal cycles) DSi can be considered as a conservative tracer for SGD because dissolution of particles, reverse weathering or biological uptake may be considered negligible with respect to the other noted sources and sinks. In this study, we consequently focus on short time-scales (hours to days). Coastal environments influenced by SGD on such short time-scales include smaller embayments, tidal channels, open beaches or rocky coastlines. Assuming that the previously mentioned processes can be neglected under short time-scales, Eq. 1 simplifies to:

$$F_{\text{SGD}} + F_{\text{diff}} + F_{\text{runoff}} = F_{\text{mix}} \quad (2)$$

Note that Eq. 2 is similar to commonly employed ^{222}Rn and Ra mass balances. DSi source and sink terms outlined in Eqs 1 and 2 are discussed in further detail below.

Dissolved silicon inputs from rainfall are usually low when compared to SGD. Concentrations between 0.5 and 15 μM were measured in rainwater in the Yellow Sea and East China Sea (Zhang et al., 2005). In the Mediterranean Sea, concentrations of DSi in rainfall range from below detection limit up to 33 μM, whereas higher concentrations are linked to episodic Saharan dust inputs (Bartoli et al., 2005).

The importance of molecular diffusion as a source of DSi will vary from site to site. Diffusive fluxes (F_{diff}) can be measured using *ex situ* or *in situ* sediment incubation experiments, if bioturbation and bioirrigation can be neglected, for example by inactivation of benthic fauna by asphyxiation (Rutgers Van Der Loeff et al., 1984; Forster and Graf, 1995). Diffusion can also be calculated based on pore water profiles of DSi from Fick's first law (Schink et al., 1974; Oehler et al., 2015; Tamborski et al., 2018).

River and surface runoff (F_{runoff}) can contain significant amounts of DSi as well as amorphous silica and solid phases which can rapidly dissolve upon estuarine mixing (Conley, 1997). Therefore, the amount of DSi transported into the coastal water column by rivers has to be carefully determined, e.g., by measuring riverine discharge and DSi concentrations, which is also required for other tracers such as ^{222}Rn or Ra. At the global (Dürr et al., 2011; Tréguer and De La Rocha, 2013), regional (Hartmann et al., 2010; Moosdorf et al., 2011), and local (Rad et al., 2007; Schopka and Derry, 2012) scale, DSi fluxes from rivers are well known and measuring methodologies are established. Obviously, close to a river, these fluxes can dominate coastal DSi fluxes. Globally, riverine DSi fluxes amount to 70 t Si per km of coastline, based on riverine Si fluxes of 5.8 Tmol Si/a (Tréguer and De La Rocha, 2013) and a global coastline of 2.3 mio km (Moosdorf et al., 2015). Offshore mixing (F_{mix}) of a tracer can be estimated by different approaches. In an embayment or an estuary where mixing is dominated by tidal forces, offshore mixing can be calculated based on a tidal prism approach (Dyer, 1973). Offshore mixing rates can also directly be measured, for example, by using an Acoustic Doppler Current Profiler (ADCP). Numerical models can be developed to estimate mixing rates and residence times. Alternatively, short-lived Ra and Rn isotopes may be used to estimate mixing with offshore waters (e.g., Burnett and Dulaiova, 2003; Moore et al., 2006). When short time-scale processes are considered (Eq. 2), the mixing loss of DSi must be well-constrained in order to properly balance DSi sources.

If the previously mentioned DSi fluxes (F_{rain}, F_{runoff}, F_{mix}, F_{diff}) into the coastal water column can be quantified or neglected, then the SGD flux can be calculated by dividing the DSi flux from SGD (F_{SGD}) with the DSi concentration in groundwater. Selection of the groundwater endmember should be based on the considerations outlined in section "DSi in Groundwater and the Subterranean Estuary."

CASE STUDIES

Case Study 1: DSi as a Tracer for SGD in a Tropical Volcanic-Carbonate Karstic Region (Southern Java, Indonesia)

The coastline of the tropical karstic region of Gunung Sewu (southern Java) is made of strongly karstified massive coral reef-limestone with intercalated clay and volcanic ash lenses (van Bemmelen, 1949; Flathe and Pfeiffer, 1965; Waltham et al., 1983; Haryono and Day, 2004). Toward the hinterland mountain ranges occur which consist mainly of sediments and volcanic deposits (a detailed geological description and geological map can be found in Oehler et al., 2018). Groundwater flows from several kilometers in the hinterland toward the coast and is enriched in DSi most likely due to the weathering of volcanic material in the hinterland, and the weathering of volcanic ash lenses during transport toward the coast. DSi enriched groundwater thus discharges through intertidal and submarine springs into the coastal ocean (Oehler et al., 2018). The regional lithology is a combination of volcanic and carbonate rocks in the hinterland and dominantly carbonate at the coast, with groundwater DSi concentrations between 200 and 400 μM with a salinity ranging from 0 to 11 (**Figure 2A**, triangles). Surface water samples taken within an embayment which receives groundwater from a single submarine spring and is not affected by surface runoff or river discharge, showed a linear inverse correlation between DSi and salinity (**Figure 2A**, gray dotted line, $R^2 = 0.84$), indicating the input of DSi from terrestrial SGD. An inverse linear correlation was also observed between $^{224}\text{Ra}_{\text{ex}}$ and salinity (**Figure 2B**, gray dotted line, $R^2 = 0.60$), with more scatter between long-lived ^{226}Ra and salinity (**Figure 2C**, gray dotted line, $R^2 = 0.03$), also indicating inputs of Ra from SGD. Fresh groundwater was low in ^{224}Ra with a concentration of 10.3 dpm 100 L^{-1}, whereas brackish groundwater was enriched in ^{224}Ra with a concentration of up to 38.7 dpm 100 L^{-1} (**Figure 2B**, triangles). ^{226}Ra was slightly enriched in brackish groundwater and highly enriched in fresh groundwater compared to seawater (**Figure 2C**).

Higher DSi concentrations in the coastal water column (139 μM) were observed during low tide and lower concentrations (65 μM) were observed during high tide (**Supplementary Material**). The tidal variations can be used in a tidal prism approach to calculate water residence times (Eq. 3 in the **Supplementary Material**) (Moore et al., 2006), which yielded a water residence time of 0.56 days. The surface water residence time value is reasonable, as the embayment is subject to diurnal tidal variations.

Submarine groundwater discharge fluxes based on the different tracer approaches were calculated based on Eq. 5 (see **Supplementary Material**) and are shown in **Table 2**. We were not able to calculate a SGD flux based on ^{226}Ra, due to the high ^{226}Ra concentrations in seawater (see **Supplementary Material**). The maximum SGD flux derived from DSi (72 cm day^{-1}) was based on the brackish groundwater endmember, and represents brackish SGD. Consequently, these results agree well with the average SGD fluxes based on $^{224}\text{Ra}_{\text{ex}}$ (65 cm day^{-1}), where the brackish groundwaters were also used as an endmember.

However, coastal water DSi concentrations were slightly lower as it would be expected from theoretical conservative mixing between fresh groundwater and seawater (**Figure 2A**, black dotted line), which indicates either an unknown source of freshwater in the coastal water column which dilutes the DSi signal, or an unknown DSi sink. Freshwater inputs into the coastal water column from rainfall can be neglected, as there was no rainfall within the sampling period. River and surface runoff is minor and can be neglected as a source of DSi as well, which is typical for karstic regions. DSi concentrations in karstic groundwaters can vary over short time scales and the full range of the groundwater DSi endmember may have not been accurately captured in this study, where samples were taken within days. Coastal water DSi concentrations may have also been partially reduced due to an uptake by marine biota (e.g., diatoms), or reverse weathering, which is however, unlikely due to the short coastal water residence times.

Case Study 2: DSi as a Tracer for SGD in a Temperate Coastal Region Protected by Barrier Islands (Spiekeroog, Southern North Sea)

Diatoms are one of the major algae groups present during spring phytoplankton blooms in the North Sea and its surrounding tidal

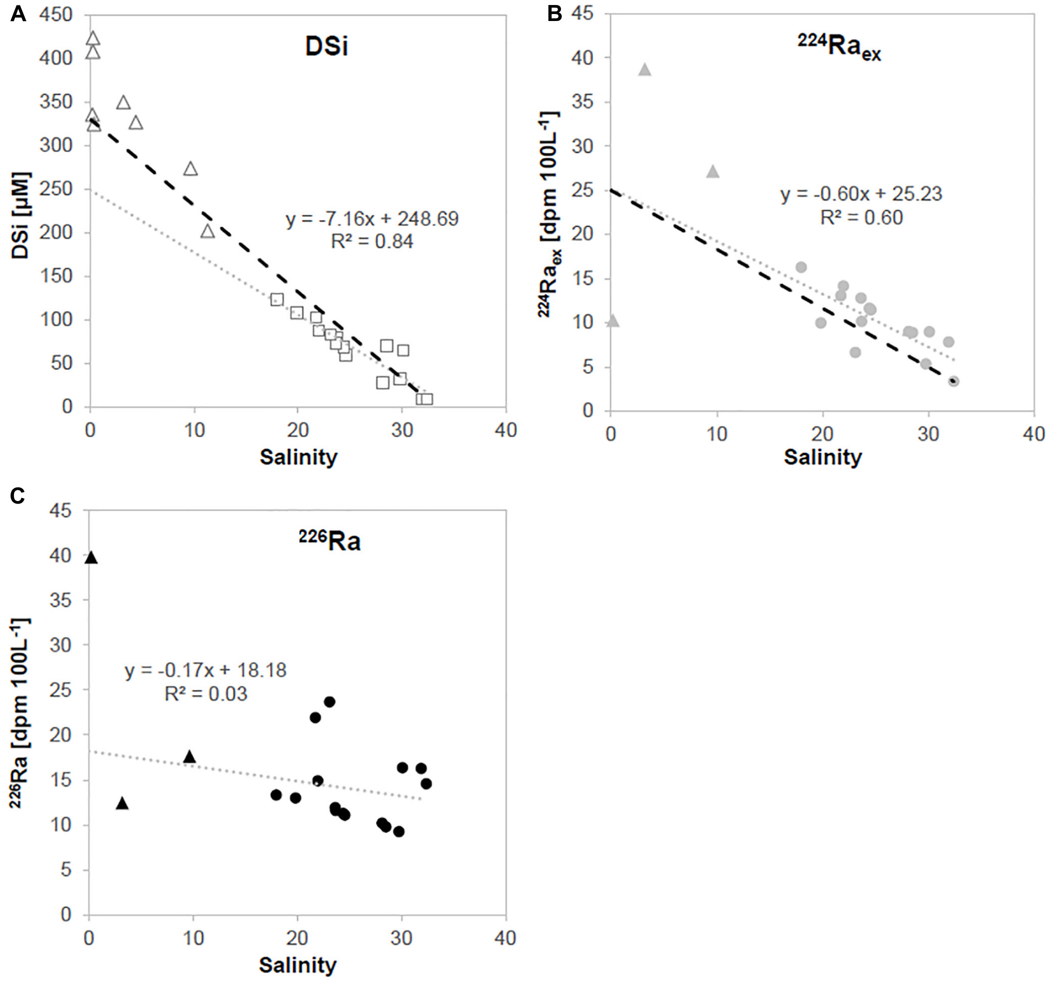

FIGURE 2 | Salinity plotted against **(A)** DSi, **(B)** ^{224}Ra$_{ex}$ and **(C)** ^{226}Ra concentrations of water samples taken in an embayment in a karstic region in southern Java. Squares and dots represent surface water column measurements and triangles represent samples taken at coastal and submarine springs. Gray dotted lines show linear correlations of samples taken from the water column, while black dotted lines indicate theoretical conservative mixing between the average groundwater concentration and seawater. Note that only selected spring samples were analyzed for Ra isotopes.

flat system (Reid et al., 1990; Schoemann et al., 1998; Meier et al., 2015; Wiltshire et al., 2015). Diatom growth and the associated DSi uptake control seasonal DSi dynamics in the water column. For example, in the Spiekeroog tidal basin DSi concentrations are high during winter (20–30 µM) and decrease strongly in the water column during the spring diatom bloom reaching concentrations close to zero (**Figure 3**; Grunwald et al., 2010; Beck and Brumsack, 2012). After the bloom, diatoms remain one of the dominant algal groups during the entire growing season (Meier et al., 2015). Furthermore, dinoflagellates, which are adapted to low nutrient concentrations and can have a siliceous skeleton, become important in summer (Meier, 2014; Wiltshire et al., 2015). Both phytoplankton species lead to a continuous DSi consumption until late autumn. The DSi pool in the water column is replenished by discharge of DSi-rich marine groundwater from the surrounding tidal flat sediments where the deposited diatom detritus is degraded (Billerbeck et al., 2006; Beck et al., 2008; Kowalski et al., 2012). Pore water advection in surface sediments (Huettel et al., 1998) leads to the release of DSi-rich pore waters, especially after the spring bloom (DSi up to 400 µM Kowalski et al., 2012). Additionally, SGD from tidal flat margin sediments (Riedel et al., 2010; Moore et al., 2011) lead to the release of groundwater enriched in DSi throughout the whole year (DSi up to 1000 µM Reckhardt et al., 2015).

TABLE 2 | SGD calculations in southern Java based on ^{224}Ra$_{ex}$, salinity and DSi mass balances.

	Salinity	DSi [µM]	^{224}Ra$_{ex}$ [dpm 100L^{-1}]
Groundwater	0–11	330 (min 202, max 423)	25.4 (min 10.3, max 38.7)
Coast	25.0	70.6	10.4
Offshore	32.4	8.5	3.3
SGD (cm day^{-1})	54	44 (min 34, max 72)	65 (min 43, max 161)

SGD fluxes are calculated based on average endmember of all coastal springs for ^{224}*Ra*$_{ex}$ *and DSi, respectively.*

The latter process occurs only around low tide when the tidal flat margins are exposed and is reflected in tidal DSi dynamics in the water column, with highest DSi concentrations around low tide (**Figure 4**; Grunwald et al., 2010). Similar to DSi, SGD transports $^{224}\mathrm{Ra}_{\mathrm{ex}}$ and $^{222}\mathrm{Rn}$ to the open water column resulting in tidal variations as well (**Figure 4**; Moore et al., 2011; Santos et al., 2015).

The tidal variations in the water column qualify DSi as tracer for SGD because additional DSi is required to obtain the enrichments measured during low tide. Given the low surface freshwater runoff (i.e., by a flood-gate) (Grunwald et al., 2010), the primary DSi source is SGD. Consequently, mass balance models can be developed to estimate SGD fluxes (Eq. 5). For the SGD estimation, a DSi endmember concentration in marine groundwater of 500 μM (Reckhardt et al., 2015) and a DSi concentration difference between tidal basin and nearshore waters of 8 μM (**Figure 4**) was assumed. Mean water volume (105×10^6 m^3) and flushing time (4 days) of the tidal basin was assessed by Stanev et al. (2003) and Moore et al. (2011), respectively. Based on DSi, the SGD flux to the Spiekeroog tidal basin amounts to about 2×10^8 L tidal-cycle^{-1}, which is in the same range of 2–4 $\times 10^8$ L tidal-cycle^{-1} as calculated by Moore et al. (2011) using Ra isotopes. This SGD flux is equivalent to 30 cm day^{-1}, assuming a tidal flat margin length of 59 km for the entire Spiekeroog tidal basin (Moore et al., 2011) and a seepage zone of 25 m (Røy et al., 2008).

We propose that at sites highly controlled by seasonal diatom growth like the coastal region of the southern North Sea, the use of DSi is restricted to certain times of the year. With the onset of the spring diatom bloom until late summer, intensive biological DSi consumption and subsequent dissolution of diatom detritus alter the water column composition (e.g., **Figure 3**). Therefore, we suggest to restrict the use of DSi as tracer for SGD to time spans with low biological activity. $^{224}\mathrm{Ra}_{\mathrm{ex}}$ may in turn be used as a tracer for SGD independent from the season (**Figure 4**).

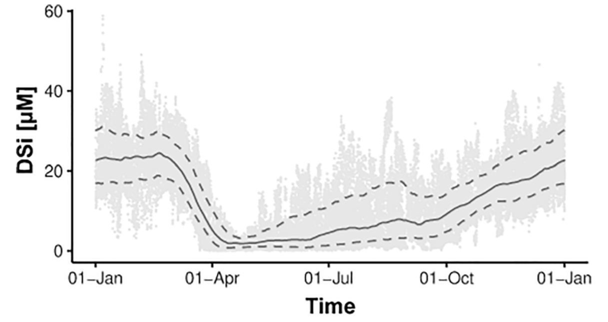

FIGURE 3 | Seasonal DSi dynamics in the water column of the Spiekeroog tidal basin. The solid line indicates the moving average of the time-dependent median including data from 2007 to 2017 and reflects typical seasonal DSi variations occurring every year. The dashed lines show the 10 and 90% quantiles.

DISCUSSION

When and Where Is DSi a Useful Tracer for SGD?

Dissolved silicon can be used as a tracer for terrestrial and marine SGD, as any water which is in contact with a sediment or aquifer matrix will be enriched in DSi with time. Some studies have used DSi as a tracer for SGD in regions impacted by a high terrestrial groundwater flow. These regions include volcanic and/or karstified carbonate rocks where a high terrestrial SGD flow occurs along conduits and cracks. For example, DSi was applied as a tracer for SGD in karstic carbonate regions such as Yucatan (Hernández-Terrones et al., 2011) and Castello, Spain (Garcia-Solsona et al., 2010b), in volcanic regions such as Hawaii (Street et al., 2008; Lubarsky et al., 2018) or Jeju island (Hwang et al., 2005) or in a mixture of volcanic and carbonate lithology's such as in southern Java (this study). Marine SGD is usually depleted in DSi in these regions (e.g., **Table 1**), and therefore DSi will either reflect brackish or fresh discharging groundwater. If brackish SGD discharges into the ocean, DSi can be used to assess the brackish fraction of SGD, in a similar way as Ra isotopes (Garcia-Solsona et al., 2010b). An SGD flux calculated on the basis of a brackish DSi groundwater endmember may thus represent a brackish SGD flux (e.g., as shown in the case study in southern Java). A fresh SGD flux should theoretically be calculated based on the DSi endmember in fresh groundwater, if conservative mixing between fresh groundwater and seawater occurs.

In tropical regions, large amounts of freshwater inputs from surface runoff and rainfall into the coastal water column further limit the applicability of salinity as a tracer for fresh SGD. DSi can consequently be a useful alternative tracer for fresh SGD. While terrestrial SGD is particularly high on small tropical islands (Zektser and Loaiciga, 1993; Moosdorf et al., 2015), only a few studies have been conducted in these regions (e.g., Matson, 1993; Kamermans et al., 2002; Knee et al., 2016; Oehler et al., 2018; Haßler et al., 2019), because they are often remote. In some instances, DSi concentrations and fluxes are reported (e.g., Johnson et al., 2008), but DSi has only rarely been used as a tracer. In southern Java, for example, the logistically challenging infrastructure (e.g., remote beaches, Ra samples needed to be exported) did not allow us to obtain large datasets for Ra (only three groundwater samples). Using DSi as an additional tracer for SGD in this setting thus allowed us to assess SGD fluxes more accurately. The comparably simple methods for measuring DSi combined with its elevated concentrations in groundwater suggest its usability as tracer for SGD in such remote locations.

In environments dominated by permeable sandy sediments DSi can also be used as tracer for SGD, as marine groundwater (or pore water) is highly enriched in DSi, for example reaching concentrations of up to 1000 μM in the tidal flat area of Spiekeroog (Reckhardt et al., 2015). In these regions DSi shows a similar tidal variability as $^{224}\mathrm{Ra}_{\mathrm{ex}}$, indicating a similar source from SGD (**Figure 4**). SGD fluxes based on DSi are in a similar range as those calculated from ^{224}Ra, indicating its suitability to quantify flux rates. However, high biological uptake rates of DSi (e.g., from pelagic or benthic siliceous phytoplankton) limit the time when DSi can be used as a tracer for SGD to periods

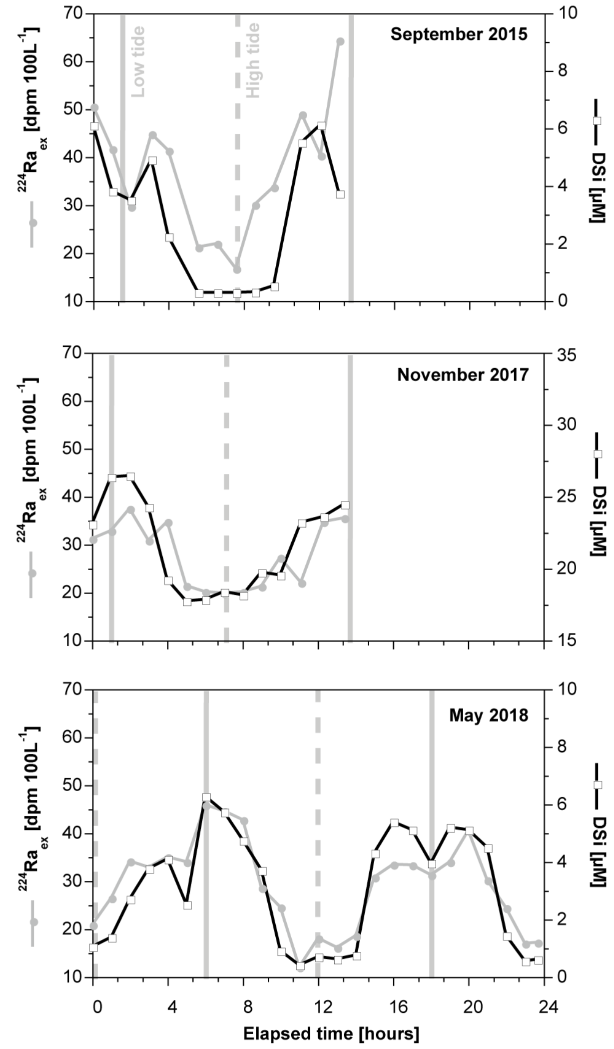

FIGURE 4 | Tidal DSi and $^{224}Ra_{ex}$ dynamics in the water column of the Spiekeroog tidal basin, with highest concentrations/activities around low tide when submarine discharge of DSi/Ra-rich groundwater is highest. The vertical solid and dashed lines indicate low tide and high tide, respectively. The water level changes smoothly depending on the tidal state. In contrast, tidal variations of DSi and $^{224}Ra_{ex}$ show a less smooth pattern because the tidal flat area consists of several tidal flats, which slightly differ in SGD fluxes and DSi endmember concentrations.

when primary productivity is low, for example due to low light availability (**Figure 3**).

Dissolved silicon can also be used in combination with other tracers such as $^{224}Ra_{ex}$ and ^{226}Ra or ^{222}Rn to calculate SGD fluxes and water residence times (e.g., Hwang et al., 2005), an approach which was successfully applied in Yeongil Bay (Kim et al., 2008), Geoje Bay (Hwang et al., 2016) and in Bangdu Bay (Hwang et al., 2005) and might be a useful tool in further SGD studies. DSi can also be useful in SGD studies if groundwater transport processes are investigated. DSi concentration gradients in the sediment can be used to identify exfiltration and infiltration patterns (Waska et al., 2019). Furthermore, if only marine SGD is investigated, simple sediment dissolution experiments can be carried out in order to estimate the residence time of marine groundwater in the sediment based on DSi groundwater concentrations (Anschutz et al., 2009).

When and Where Is DSi Not Applicable as a Tracer for SGD?

The use of DSi as a tracer for SGD is complicated if unknown or unquantifiable sources or sinks of DSi exist. Inputs of particulate Si can occur from rivers and atmospheric deposition, which need to be considered as particles can partly dissolve and release DSi into the water column. Reverse weathering, adsorption to Fe-oxides, precipitation of amorphous Al-Si phases and biological uptake can reduce DSi concentrations in surface sediments and in the water column. In SGD studies over larger spatial (e.g., shelf) or temporal scales (weeks to years) (Lee et al., 2009; Tamborski et al., 2018), the quantification of the previously named DSi sources and sinks and likewise its applicability as a tracer for SGD will become difficult.

Biological uptake depends on various factors such as the growing speed and abundance of DSi incorporating organisms, the availability of other nutrients, temperature and light (e.g., Abreu et al., 1994; DeMaster et al., 1996; Ragueneau et al., 2002; Krause et al., 2011). In many coastal regions, algae blooms such as diatoms follow a seasonal pattern (van Beusekom and Diel-Christiansen, 2009; Grunwald et al., 2010). Using DSi as a tracer for SGD may not be appropriate in these regions if biological uptake of DSi from the water column and pore waters in surface sediments is much higher when compared to inputs via SGD. DSi is for example depleted during spring phytoplankton blooms in the southern North Sea, whereby it acts as a limiting nutrient for primary producers. Biological uptake rates of DSi are consequently high during this time and difficult to quantify. During and after the deposition of diatoms at the seafloor, dissolution rates of biogenic opal in surface sediments are usually high which leads to a high efflux of DSi into the water column (Ehrenhauss et al., 2004; Oehler et al., 2015) and high DSi concentrations in groundwater (or pore water) (Reckhardt et al., 2015). During these times, the end-member concentration of DSi in groundwater will be extraordinarily high and has to be carefully determined. In the southern North Sea it will thus be more difficult to apply DSi as a tracer for SGD during and after phytoplankton blooms in comparison to periods when primary productivity is low (Beusekom and Diel-Christiansen, 2007). In many coastal regions the timing of phytoplankton blooms are well known, and thus appropriate times can be selected during which measurements should be carried out. In addition, it can be useful to determine the phytoplankton community composition and abundance if DSi is used as a tracer for SGD. Similar to other geochemical tracers, DSi cannot be used as a tracer of SGD if the DSi endmember is poorly constrained. Total SGD is composed of several different flow paths driven by a variety of different forcing mechanisms (Santos et al., 2012). In volcanic and karstic environments, defining the SGD DSi endmember may be relatively straightforward (e.g., **Table 1**). But in well-developed carbonate karstic aquifers, very low DSi concentrations may occur in groundwater, especially under high flow conditions. Furthermore, in lithologic complex environments, DSi endmember concentrations can vary between flow paths. For example, SGD driven by water exchange between a lagoon and the sea will have a unique DSi endmember different from that of seawater circulation through the permeable beach-face (Tamborski et al., 2019). Recently recharged groundwaters will have lower DSi concentrations compared to older, deeper groundwaters.

CONCLUSION

We herein assess DSi as a tracer for SGD and which boundary conditions need to be considered. DSi becomes enriched in groundwater due to biogenic silica dissolution and water-rock interactions, and can reach a transient steady-state equilibrium between dissolution and reprecipitation with time. Therefore, groundwaters and pore waters are usually enriched in DSi when compared to surface waters, which makes DSi a useful tracer for terrestrial and marine SGD. Typical DSi concentrations in terrestrial and marine groundwater can be described depending on lithology of the respective aquifer: extrusive igneous, carbonate, sandstone, granite, shale and complex. Carbonate karst and volcanic regions promote a high terrestrial groundwater flow, where DSi works well as a tracer for terrestrial and brackish SGD. In other regions with complex lithologies (mixtures of sand and clay), such as coastal areas of the North Sea, DSi can be used as a tracer for marine SGD (e.g., forced by tidal pumping), due to the dissolution of lithogenic particles and siliceous ooze in the sediment. One of the largest constraints in using DSi as a tracer for SGD is its non-conservative behavior, especially due to biological uptake by diatoms and other primary producers. Therefore, DSi cannot be used as a tracer for SGD if large amounts of DSi are taken up by algae blooms in the area studied. Determining the phytoplankton community composition and abundance, or a conservative mixing line between salinity and DSi may help researchers to understand if the conditions are suitable to use DSi as a tracer for SGD. Furthermore, DSi can most likely not be used as a tracer for SGD over larger temporal (longer than days) and spatial scales, as it will become difficult to quantify all sources and sinks of DSi over larger scales. DSi can easily be sampled and transported; analyses are in general very cost effective and have a small analytical error. State of the art analytical methods allow precise DSi measurements with small sampling volumes of less than 1 mL. This allows endmember sampling in pore waters and groundwater even on a small vertical scale in the sediment, which has been suggested to be necessary for a representative SGD end-member (Cook et al., 2018). Future SGD studies should consider using DSi as an additional tracer to compliment ^{222}Rn or Ra investigations.

DATA AVAILABILITY

All datasets generated for this study are included in the manuscript and/or the **Supplementary Files**.

AUTHOR CONTRIBUTIONS

MB, RN, CM, BS, and JA collected data for case study 2 and wrote the section "DSi as a Tracer for SGD in a Temperate Coastal Region Protected by Barrier Islands (Spiekeroog, Southern North Sea)." JT and SR contributed with data and interpretation of sections "DSi as an Indicator for Groundwater Transport Processes" and "DSi as a Tracer for SGD in Coastal Waters" and wrote the section "DSi as an Indicator for Groundwater Transport Processes." TO, NM, and BS collected data for section "DSi as a Tracer for SGD in a Tropical Volcanic-Carbonate Karstic Region (Southern Java, Indonesia)." All authors contributed with the interpretation, writing and editing of the manuscript. TO compiled everything and wrote largest parts of sections "Introduction," "DSi as a Tracer for SGD in Coastal Waters," "DSi as a Tracer for SGD in a Tropical Volcanic-Carbonate Karstic Region (Southern Java, Indonesia)," "Discussion" and "Conclusion."

FUNDING

TO, NM, and the presented case study 1 were funded through the BMBF junior research group SGD-NUT (grant #01LN1307A). Open access publication fees are paid by Leibniz-Centre for Tropical Marine Research internal funds. The presented case study 2 was financially supported by the DFG Research Group "BioGeoChemsitry of Tidal Flats", the Ph.D. Research Training Group "The ecology of molecules" funded by the Ministry for Science and Culture of Lower Saxony, and the Institute for Chemistry and Biology of the Marine Environment, University of Oldenburg.

ACKNOWLEDGMENTS

We thank A.-S. Rupp and T. Wischermann for assistance during sampling as well as J. Freund and P. Hähnel for providing **Figure 3**. The crew of the FK Senckenberg is gratefully acknowledged.

SUPPLEMENTARY MATERIAL

The Supplementary Material for this article can be found online at: https://www.frontiersin.org/articles/10.3389/fmars.2019.00563/full#supplementary-material

REFERENCES

Abreu, P. C., Odebrecht, C., and González, A. (1994). Particulate and dissolved phytoplankton production of the patos lagoon estuary, southern Brazil: comparison of methods and influencing factors. *J. Plankton Res.* 16, 737–753. doi: 10.1093/plankt/16.7.737

Advocat, T., Chouchan, J. L., Crovisier, J. L., Guy, C., Daux, V., Jegou, C., et al. (1998). Borosilicate nuclear waste glass alteration kinetics: chemical inhibition and affinity control. *Mater. Res. Soc. Symp. Proc.* 506, 63–70. doi: 10.1557/PROC-506-63

Anschutz, P., Smith, T., Mouret, A., Deborde, J., Bujan, S., Poirier, D., et al. (2009). Tidal sands as biogeochemical reactors. *Estuar. Coast. Shelf Sci.* 84, 84–90. doi: 10.1016/j.ecss.2009.06.015

Bartoli, G., Migon, C., and Losno, R. (2005). Atmospheric input of dissolved inorganic phosphorus and silicon to the coastal northwestern mediterranean sea: fluxes, variability and possible impact on phytoplankton dynamics. *Deep Sea Res. Part I Oceanogr. Res. Pap.* 52, 2005–2016. doi: 10.1016/J.DSR.2005.06.006

Beck, A. J., and Cochran, M. A. (2013). Controls on solid-solution partitioning of radium in saturated marine sands. *Mar. Chem.* 156, 38–48. doi: 10.1016/J.MARCHEM.2013.01.008

Beck, M., and Brumsack, H.-J. (2012). Biogeochemical cycles in sediment and water column of the Wadden Sea: the example spiekeroog Island in a regional context. *Ocean Coast. Manag.* 68, 102–113. doi: 10.1016/j.ocecoaman.2012.05.026

Beck, M., Dellwig, O., Liebezeit, G., Schnetger, B., and Brumsack, H.-J. (2008). Spatial and seasonal variations of sulphate, dissolved organic carbon, and nutrients in deep pore waters of intertidal flat sediments. *Estuar. Coast. Shelf Sci.* 79, 307–316. doi: 10.1016/j.ecss.2008.04.007

Beusekom, J. E. E., and Diel-Christiansen, S. (2007). Global change and the biogeochemistry of the north sea: the possible role of phytoplankton and phytoplankton grazing. *Int. J. Earth Sci.* 98, 269–280. doi: 10.1007/s00531-007-0233-8

Billerbeck, M., Werner, U., Bosselmann, K., Walpersdorf, E., and Huettel, M. (2006). Nutrient release from an exposed intertidal sand flat. *Mar. Ecol. Prog. Ser.* 316, 35–51. doi: 10.3354/meps316035

Bluth, G. J. S., and Kump, L. R. (1994). Lithologic and climatologic controls of river chemistry. *Geochim. Cosmochim. Acta* 58, 2341–2359. doi: 10.1016/0016-7037(94)90015-9

Brzezinski, M. A. (1985). The Si:C:N ratio of marine diatoms: interspecific variability and the effect of some environmental variables. *J. Phycol.* 21, 347–357. doi: 10.1111/j.0022-3646.1985.00347.x

Burnett, W., and Dulaiova, H. (2003). Estimating the dynamics of groundwater input into the coastal zone via continuous radon-222 measurements. *J. Environ. Radioact.* 69, 21–35. doi: 10.1016/s0265-931x(03)00084-5

Burnett, W. C., Bokuniewicz, H., Huettel, M., Moore, W. S., and Taniguchi, M. (2003). Groundwater and pore water inputs to the coastal zone. *Biogeochemistry* 66, 3–33. doi: 10.1023/B:BIOG.0000006066.21240.53

Charbonnier, C., Anschutz, P., Poirier, D., Bujan, S., and Lecroart, P. (2013). Aerobic respiration in a high-energy sandy beach. *Mar. Chem.* 155, 10–21. doi: 10.1016/j.marchem.2013.05.003

Conley, D. J. (1997). Riverine contribution of biogenic silica to the oceanic silica budget. *Limnol. Oceanogr.* 42, 774–777. doi: 10.4319/lo.1997.42.4.0774

Cook, P. G., Rodellas, V., and Stieglitz, T. C. (2018). Quantifying surface water, porewater, and groundwater interactions using tracers: tracer fluxes, water fluxes, and end-member concentrations. *Water Resour. Res.* 54, 2452–2465. doi: 10.1002/2017WR021780

Daux, V., Guy, C., Advocat, T., Crovisier, J.-L., and Stille, P. (1997). Kinetic aspects of basaltic glass dissolution at 90°C: role of aqueous silicon and aluminium. *Chem. Geol.* 142, 109–126. doi: 10.1016/S0009-2541(97)00079-X

DeMaster, D. J. (2002). The accumulation and cycling of biogenic silica in the Southern Ocean: revisiting the marine silica budget. *Deep Sea Res. Part II Top. Stud. Oceanogr.* 49, 3155–3167. doi: 10.1016/S0967-0645(02)00076-0

DeMaster, D. J. (2003). The diagenesis of biogenic silica: chemical transformations occurring in the water column, seabed, and crust. *Treat. Geochimica.* 7, 87–98. doi: 10.1016/B978-0-08-095975-7.00704-X

DeMaster, D. J., Ragueneau, O., and Nittrouer, C. A. (1996). Preservation efficiencies and accumulation rates for biogenic silica and organic C, N, and P in high-latitude sediments: the ross sea. *J. Geophys. Res. Ocean.* 101, 18501–18518. doi: 10.1029/96JC01634

Dixit, S., and Van Cappellen, P. (2002). Surface chemistry and reactivity of biogenic silica. *Geochim. Cosmochim. Acta* 66, 2559–2568. doi: 10.1016/S0016-7037(02)00854-2

Dulaiova, H., Camilli, R., Henderson, P. B., and Charette, M. A. (2010). Coupled radon, methane and nitrate sensors for large-scale assessment of groundwater discharge and non-point source pollution to coastal waters. *J. Environ. Radioact.* 101, 553–563. doi: 10.1016/j.jenvrad.2009.12.004

Dürr, H., Laruelle, G., van Kempen, C., and Slomp, C. (2011). Worldwide typology of nearshore coastal systems: defining the estuarine filter of river inputs to the oceans. *Estuaries Coast.* 34, 441–458. doi: 10.1007/s12237-011-9381-y

Dyer, K. (1973). *Estuaries: a Physical Introduction*. London: John Wiley.

Ehlert, C., Reckhardt, A., Greskowiak, J., Liguori, B. T. P., Böning, P., Paffrath, R., et al. (2016). Transformation of silicon in a sandy beach ecosystem: insights from stable silicon isotopes from fresh and saline groundwaters. *Chem. Geol.* 440, 207–218. doi: 10.1016/J.CHEMGEO.2016.07.015

Ehrenhauss, S., Witte, U., Janssen, F., and Huettel, M. (2004). Decomposition of diatoms and nutrient dynamics in permeable north sea sediments. *Cont. Shelf Res.* 24, 721–737. doi: 10.1016/J.CSR.2004.01.002

Fanning, K. A., Breland, J. A., and Byrne, R. H. (1982). Radium-226 and radon-222 in the coastal waters of west Florida: high concentrations and atmospheric degassing. *Science* 215, 667–670. doi: 10.1126/science.215.4533.667

Flathe, H., and Pfeiffer, D. (1965). Grundzüge der geomorpholgie, geologie und hydrogeologie im karstgebiet gunung sewu (Java, Indonesien). *Geol. Jahrb. B* 83, 533–562.

Forster, S., and Graf, G. (1995). Impact of irrigation on oxygen flux into the sediment: intermittent pumping by callianassa subterranea and "piston-pumping" by *Lanice Conchilega*. *Mar. Biol.* 123, 335–346. doi: 10.1007/bf00353625

Garcia-Solsona, E., Garcia-Orellana, J., Masqué, P., Garcés, E., Radakovitch, O., Mayer, A., et al. (2010a). An assessment of karstic submarine groundwater and associated nutrient discharge to a Mediterranean coastal area (Balearic Islands, Spain) using radium isotopes. *Biogeochemistry* 97, 211–229. doi: 10.1007/s10533-009-9368-y

Garcia-Solsona, E., Garcia-Orellana, J., Masqué, P., Rodellas, V., Mejías, M., Ballesteros, B., et al. (2010b). Groundwater and nutrient discharge through karstic coastal springs (Castelló, Spain). *Biogeosciences* 7, 2625–2638. doi: 10.5194/bg-7-2625-2010

Gislason, S. R., and Oelkers, E. H. (2003). Mechanism, rates, and consequences of basaltic glass dissolution: II. an experimental study of the dissolution rates of basaltic glass as a function of pH and temperature. *Geochim. Cosmochim. Acta* 67, 3817–3832. doi: 10.1016/S0016-7037(00)00176-5

Grunwald, M., Dellwig, O., Kohlmeier, C., Kowalskic, N., Becka, M., Badewiena, T. H., et al. (2010). Nutrient dynamics in a back barrier tidal basin of the Southern North Sea: time-series, model simulations, and budget estimates. *J. Sea Res.* 64, 199–212. doi: 10.1016/j.seares.2010.02.008

Hartmann, J., Jansen, N., Dürr, H. H., Harashima, A., Okubo, K., and Kempe, S. (2010). Predicting riverine dissolved silica fluxes to coastal zones from a hyperactive region and analysis of their first-order controls. *Int. J. Earth Sci.* 99, 207–230. doi: 10.1007/s00531-008-0381-5

Haryono, E., and Day, M. (2004). Landform differentiation within the Gunung Kidul Kegelkarst, Java, Indonesia. *J. Cave Karst Stud.* 66, 62–69.

Haßler, K., Dähnke, K., Kölling, M., Sichoix, L., Nickl, A.-L., and Moosdorf, N. (2019). Provenance of nutrients in submarine fresh groundwater discharge on Tahiti and Moorea, French Polynesia. *Appl. Geochem.* 100, 181–189. doi: 10.1016/J.APGEOCHEM.2018.11.020

Hernández-Terrones, L., Rebolledo-Vieyra, M., Merino-Ibarra, M., Soto, M., Le-Cossec, A., and Monroy-Ríos, E. (2011). Groundwater pollution in a karstic region (NE Yucatan): baseline nutrient content and flux to coastal ecosystems. *Water Air Soil Pollut.* 218, 517–528. doi: 10.1007/s11270-010-0664-x

Horton, T. W., Chamberlain, C. P., Fantle, M., and Blum, J. D. (1999). Chemical weathering and lithologic controls of water chemistry in a high-elevation river system: clark's fork of the yellowstone river, wyoming and montana. *Water Resour. Res.* 35, 1643–1655. doi: 10.1029/1998WR900103

Huettel, M., Ziebis, W., Forster, S., and Luther, G. W. (1998). Advective transport affecting metal and nutrient distributions and interfacial fluxes in permeable sediments. *Geochim. Cosmochim. Acta* 62, 613–631. doi: 10.1016/S0016-7037(97)00371-2

Hurd, D. C. (1973). Interactions of biogenic opal, sediment and seawater in the Central Equatorial Pacific. *Geochim. Cosmochim. Acta* 37, 2257–2282. doi: 10.1016/0016-7037(73)90103-8

Hwang, D., Lee, Y., and Kim, G. (2005). Large submarine groundwater discharge and benthic eutrophication in Bangdu Bay on volcanic Jeju Island, Korea. *Limnol. Oceanogr.* 50, 1393–1403. doi: 10.4319/lo.2005.50.5.1393

Hwang, D.-W., Lee, I.-S., Choi, M., and Kim, T.-H. (2016). Estimating the input of submarine groundwater discharge (SGD) and SGD-derived nutrients in Geoje Bay, Korea using 222Rn-Si mass balance model. *Mar. Pollut. Bull.* 110, 119–126. doi: 10.1016/J.MARPOLBUL.2016.06.073

Jacobson, A. D., Blum, J. D., Chamberlain, C. P., Craw, D., and Koons, P. O. (2003). Climatic and tectonic controls on chemical weathering in the New Zealand Southern Alps. *Geochim. Cosmochim. Acta* 67, 29–46. doi: 10.1016/S0016-7037(02)01053-0

Jeandel, C., and Oelkers, E. H. (2015). The influence of terrigenous particulate material dissolution on ocean chemistry and global element cycles. *Chem. Geol.* 395, 50–66. doi: 10.1016/j.chemgeo.2014.2014.12.001

Johnson, A. G., Glenn, C. R., Burnett, W. C., Peterson, R. N., and Lucey, P. G. (2008). Aerial infrared imaging reveals large nutrient-rich groundwater inputs to the ocean. *Geophys. Res. Lett.* 35:L15606. doi: 10.1029/2008GL034574

Jones, M. T., Pearce, C. R., Jeandel, C., Gislason, S. R., Eiriksdottir, E. S., Mavromatis, V., et al. (2012). Riverine particulate material dissolution as a significant flux of strontium to the oceans. *Earth Planet. Sci. Lett.* 35, 51–59. doi: 10.1016/j.epsl.2012.08.040

Kamermans, P., Hemminga, M. A., Tack, J. F., Mateo, M. Á, Marbà, N., Mtolera, M., et al. (2002). Groundwater effects on diversity and abundance of lagoonal seagrasses in Kenya and on Zanzibar Island (East Africa). *Mar. Ecol. Prog. Ser* 231, 75–83. doi: 10.3354/meps231075

Khalil, K., Rabouille, C., Gallinari, M., Soetaert, K., DeMaster, D. J., and Ragueneau, O. (2007). Constraining biogenic silica dissolution in marine sediments: a comparison between diagenetic models and experimental dissolution rates. *Mar. Chem.* 106, 223–238. doi: 10.1016/j.marchem.2006.12.004

Kim, G., Ryu, J.-W., and Hwang, D.-W. (2008). Radium tracing of submarine groundwater discharge (SGD) and associated nutrient fluxes in a highly-permeable bed coastal zone, Korea. *Mar. Chem.* 109, 307–317. doi: 10.1016/J.MARCHEM.2007.07.002

Kim, G., Ryu, J.-W., Yang, H.-S., and Yun, S.-T. (2005). Submarine groundwater discharge (SGD) into the Yellow Sea revealed by 228Ra and 226Ra isotopes: implications for global silicate fluxes. *Earth Planet. Sci. Lett.* 237, 156–166. doi: 10.1016/J.EPSL.2005.06.011

Knee, K. L., Crook, E. D., Hench, J. L., Leichter, J. J., and Paytan, A. (2016). Assessment of submarine groundwater discharge (SGD) as a source of dissolved radium and nutrients to Moorea (French Polynesia) Coastal Waters. *Estuaries Coast.* 39, 1651–1668. doi: 10.1007/s12237-016-0108-y

Kowalski, N., Dellwig, O., Beck, M., Gräwea, U., Neubertc, N., Näglerc, T. F., et al. (2013). Pelagic molybdenum concentration anomalies and the impact of sediment resuspension on the molybdenum budget in two tidal systems of the North Sea. *Geochim. Cosmochim. Acta* 119, 198–211. doi: 10.1016/J.GCA.2013.05.046

Kowalski, N., Dellwig, O., Beck, M., Grunwald, M., Dürselend, C.-D., Badewienb, T. H., et al. (2012). A comparative study of manganese dynamics in the water column and sediments of intertidal systems of the North Sea. *Estuar. Coast. Shelf Sci.* 100, 3–17. doi: 10.1016/j.ecss.2011.03.011

Krause, J. W., Brzezinski, M. A., Baines, S. B., Collier, J. L., Twining, B. S., and Ohnemus, D. C. (2017). Picoplankton contribution to biogenic silica stocks and production rates in the Sargasso Sea. *Global Biogeochem. Cycles* 31, 762–774. doi: 10.1002/2017GB005619

Krause, J. W., Nelson, D. M., and Brzezinski, M. A. (2011). Biogenic silica production and the diatom contribution to primary production and nitrate uptake in the eastern equatorial Pacific Ocean. *Deep Sea Res. Part II Top. Stud. Oceanogr.* 58, 434–448. doi: 10.1016/J.DSR2.2010.08.010

Lecher, A., and Mackey, K. (2018). Synthesizing the effects of submarine groundwater discharge on marine biota. *Hydrology* 5:60. doi: 10.3390/hydrology5040060

Lecher, A. L., Chien, C.-T., and Paytan, A. (2016). Submarine groundwater discharge as a source of nutrients to the North Pacific and Arctic coastal ocean. *Mar. Chem.* 186, 167–177. doi: 10.1016/J.MARCHEM.2016.09.008

Lee, C. M., Jiao, J. J., Luo, X., and Moore, W. S. (2012). Estimation of submarine groundwater discharge and associated nutrient fluxes in Tolo Harbour, Hong Kong. *Sci. Total Environ.* 433, 427–433. doi: 10.1016/J.SCITOTENV.2012.06.073

Lee, Y.-W., Hwang, D.-W., Kim, G., Lee, W.-C., and Oh, H.-T. (2009). Nutrient inputs from submarine groundwater discharge (SGD) in Masan Bay, an embayment surrounded by heavily industrialized cities, Korea. *Sci. Total Environ.* 407, 3181–3188. doi: 10.1016/J.SCITOTENV.2008.04.013

Loucaides, S., Behrends, T., and Van Cappellen, P. (2010). Reactivity of biogenic silica: surface versus bulk charge density. *Geochim. Cosmochim. Acta* 74, 517–530. doi: 10.1016/j.gca.2009.10.038

Loucaides, S., Van Cappellen, P., and Behrends, T. (2008). Dissolution of biogenic silica from land to ocean: role of salinity and pH. *Limnol. Oceanogr.* 53, 1614–1621. doi: 10.4319/lo.2008.53.4.1614

Loucaides, S., van Cappellen, P., Roubeix, V., Moriceau, B., and Ragueneau, O. (2012). Controls on the recycling and preservation of biogenic silica from biomineralization to burial. *Silicon* 4, 7–22. doi: 10.1007/s12633-011-9092-9

Lubarsky, K. A., Silbiger, N. J., and Donahue, M. J. (2018). Effects of submarine groundwater discharge on coral accretion and bioerosion on two shallow reef flats. *Limnol. Oceanogr.* 63, 1660–1676. doi: 10.1002/lno.10799

Luo, X., Jiao, J. J., Moore, W. S., and Lee, C. M. (2014). Submarine groundwater discharge estimation in an urbanized embayment in Hong Kong via short-lived radium isotopes and its implication of nutrient loadings and primary production. *Mar. Pollut. Bull.* 82, 144–154. doi: 10.1016/J.MARPOLBUL.2014.03.005

Mackin, J. E., and Aller, R. C. (1984). Dissolved Al in sediments and waters of the East China Sea: implications for authigenic mineral formation. *Geochim. Cosmochim. Acta* 48, 281–297. doi: 10.1016/0016-7037(84)90251-5

Matson, E. A. (1993). Nutrient flux through soils and aquifers to the coastal zone of Guam (Mariana Islands). *Limnol. Oceanogr.* 38, 361–371. doi: 10.4319/lo.1993.38.2.0361

Meier, S. (2014). *Spatio Temporal Turnover Of A Phytoplankton Meta Community In a Natural Coastal System*. Ph.D thesis, University of Oldenburg, Oldenburg.

Meier, S., Muijsers, F., Beck, M., Badewien, T. H., and Hillebrand, H. (2015). Dominance of the non-indigenous diatom Mediopyxis helysia in Wadden Sea phytoplankton can be linked to broad tolerance to different Si and N supplies. *J. Sea Res.* 95, 36–44. doi: 10.1016/j.seares.2014.10.001

Michalopoulos, P., and Aller, R. C. (2004). Early diagenesis of biogenic silica in the Amazon delta: alteration, authigenic clay formation, and storage. *Geochim. Cosmochim. Acta* 68, 1061–1085. doi: 10.1016/j.gca.2003.07.018

Moore, W. (2010). The effect of submarine groundwater discharge on the ocean. *Ann. Rev. Mar. Sci.* 2, 59–88. doi: 10.1146/annurev-marine-120308-081019

Moore, W. S., Beck, M., Riedel, T., Rutgers van der Loeff, M., Dellwig, O., et al. (2011). Radium-based pore water fluxes of silica, alkalinity, manganese, DOC, and uranium: a decade of studies in the german wadden sea. *Geochim. Cosmochim. Acta* 75, 6535–6555. doi: 10.1016/J.GCA.2011.08.037

Moore, W. S., Blanton, J. O., and Joye, S. B. (2006). Estimates of flushing times, submarine groundwater discharge, and nutrient fluxes to Okatee Estuary, South Carolina. *J. Geophys. Res.* 111:C09006. doi: 10.1029/2005JC003041

Moore, W. S., and Reid, D. F. (1973). Extraction of radium from natural waters using manganese-impregnated acrylic fibers. *J. Geophys. Res.* 78, 8880–8886. doi: 10.1029/JC078i036p08880

Moosdorf, N., Hartmann, J., and Lauerwald, R. (2011). Changes in dissolved silica mobilization into river systems draining North America until the period 2081–2100. *J. Geochem. Explor.* 110, 31–39. doi: 10.1016/J.GEXPLO.2010.09.001

Moosdorf, N., and Oehler, T. (2017). Societal use of fresh submarine groundwater discharge: an overlooked water resource. *Earth Sci. Rev.* 171, 338–348. doi: 10.1016/J.EARSCIREV.2017.06.006

Moosdorf, N., Stieglitz, T., Waska, H., Dürr, H. H., and Hartmann, J. (2015). Submarine groundwater discharge from tropical islands: a review. *Grundwasser* 20, 53–67. doi: 10.1007/s00767-014-0275-3

Morin, G. P., Vigier, N., and Verney-Carron, A. (2015). Enhanced dissolution of basaltic glass in brackish waters: impact on biogeochemical cycles. *Earth Planet. Sci. Lett.* 417, 1–8. doi: 10.1016/j.epsl.2015.02.005

Oehler, T., Eiche, E., Putra, D., Adyasari, D., Hennig, H., Mallast, U., et al. (2018). Seasonal variability of land-ocean groundwater nutrient fluxes from a tropical karstic region (southern Java, Indonesia). *J. Hydrol.* 565, 662–671. doi: 10.1016/J.JHYDROL.2018.08.077

Oehler, T., Schlüter, M., and Schückel, U. (2015). Seasonal dynamics of the biogenic silica cycle in surface sediments of the Helgoland Mud Area (southern North Sea). *Cont. Shelf Res.* 107, 103–114. doi: 10.1016/j.csr.2015.07.016

Oelkers, E. H., and Gislason, S. R. (2001). The mechanism, rates and consequences of basaltic glass dissolution: i. an experimental study of the dissolution rates of basaltic glass as a function of aqueous al, si and oxalic acid concentration at 25°C and pH = 3 and 11. *Geochim. Cosmochim. Acta* 65, 3671–3681. doi: 10.1016/S0016-7037(01)00664-0

Oelkers, E. H., Jones, M. T., Pearce, C. R., Jeandel, C., Eiriksdottir, E. S., and Gislason, S. R. (2012). Riverine particulate material dissolution in seawater and its implications for the global cycles of the elements. *Comptes Rendus Geosci.* 344, 646–651. doi: 10.1016/j.crte.2012.08.005

Onodera, S., Saito, M., Hayashi, M., and Sawano, M. (2007). Nutrient dynamics with groundwater-seawater interactions in a beach slope of a steep island, western Japan. *IAHS Publ.* 312:150.

Rad, S. D., Allègre, C. J., and Louvat, P. (2007). Hidden erosion on volcanic islands. *Earth Planet. Sci. Lett.* 262, 109–124. doi: 10.1016/j.epsl.2007.07.019

Ragueneau, O., Chauvaud, L., Leynaert, A., Thouzeau, G., Paulet, Y.-M., Bonnet, S., et al. (2002). Direct evidence of a biologically active coastal silicate pump: ecological implications. *Limnol. Oceanogr.* 47, 1849–1854. doi: 10.4319/lo.2002.47.6.1849

Rahman, S., Tamborski, J. J., Charette, M. A., and Cochran, J. K. (2019). Dissolved silica in the subterranean estuary and the impact of submarine groundwater discharge on the global marine silica budget. *Mar. Chem.* 208, 29–42. doi: 10.1016/J.MARCHEM.2018.11.006

Reckhardt, A., Beck, M., Seidel, M., Riedel, T., Wehrmann, A., Bartholom, A., et al. (2015). Carbon, nutrient and trace metal cycling in sandy sediments: a comparison of high-energy beaches and backbarrier tidal flats. *Estuar. Coast. Shelf Sci.* 159, 1–14. doi: 10.1016/j.ecss.2015.03.025

Reid, P. C., Lancelot, C., Gieskes, W. W. C., Hagmeier, E., and Weichart, G. (1990). Phytoplankton of the North Sea and its dynamics: a review. *Netherlands J. Sea Res.* 26, 295–331. doi: 10.1016/0077-7579(90)90094-W

Rengarajan, R., and Sarma, V. V. S. S. (2015). Submarine groundwater discharge and nutrient addition to the coastal zone of the Godavari estuary. *Mar. Chem.* 172, 57–69. doi: 10.1016/J.MARCHEM.2015.03.008

Riedel, T., Lettmann, K., Beck, M., and Brumsack, H.-J. (2010). Tidal variations in groundwater storage and associated discharge from an intertidal coastal aquifer. *J. Geophys. Res.* 115:C04013. doi: 10.1029/2009JC005544

Røy, H., Lee, J. S., Jansen, S., and de Beer, D. (2008). Tide-driven deep pore-water flow in intertidal sand flats. *Limnol. Oceanogr.* 53, 1521–1530. doi: 10.4319/lo.2008.53.4.1521

Rutgers Van Der Loeff, M. M., Anderson, L. G., Hall, P. O., Iversfeldt, A., Josefson, A. B., Sundby, B., et al. (1984). The asphyxiation technique: an approach to distinguishing between molecular diffusion and biologically mediated transport at the sediment-water interface. *Limnol. Oceanogr.* 29, 675–686. doi: 10.4319/lo.1984.29.4.0675

Santos, I. R., Beck, M., Brumsack, H.-J., Maher, D. T., Dittmar, T., Waska, H., et al. (2015). Porewater exchange as a driver of carbon dynamics across a terrestrial-marine transect: insights from coupled 222Rn and pCO2 observations in the German wadden sea. *Mar. Chem.* 171, 10–20. doi: 10.1016/j.marchem.2015.02.005

Santos, I. R., Eyre, B. D., and Huettel, M. (2012). The driving forces of porewater and groundwater flow in permeable coastal sediments: a review. *Estuar. Coast. Shelf Sci.* 98, 1–15. doi: 10.1016/J.ECSS.2011.10.024

Schink, D. R., Fanning, K. A., and Pilson, M. E. Q. (1974). Dissolved silica in the upper pore waters of the Atlantic Ocean floor. *J. Geophys. Res.* 79, 2243–2250. doi: 10.1029/JC079i015p02243

Schink, D. R., Guinasso, N. L., and Fanning, K. A. (1975). Processes affecting the concentration of silica at the sediment-water interface of the Atlantic Ocean. *J. Geophys. Res.* 80, 3013–3031. doi: 10.1029/jc080i021p03013

Schoemann, V., deBarr, H. J. W., de Jong, J. T. M., and Lancelot, C. (1998). Effects of phytoplankton blooms of the cycling of manganese and iron in coastal waters. *Limnol. Oceanogr.* 43, 1427–1441. doi: 10.4319/lo.1998.43.7.1427

Schopka, H. H., and Derry, L. A. (2012). . Chemical weathering fluxes from volcanic islands and the importance of groundwater: the Hawaiian example. *Earth Planet. Sci. Lett.* 339–340, 67–78. doi: 10.1016/j.epsl.2012.05.028

Seidel, M., Beck, M., Greskowiak, J., Riedel, T., Waska, H., Suryaputra, I. G. N. A., et al. (2015). Benthic-pelagic coupling of nutrients and dissolved organic matter composition in an intertidal sandy beach. *Mar. Chem.* 176, 150–163. doi: 10.1016/J.MARCHEM.2015.08.011

Slomp, C., and Van Cappellen, P. (2004). Nutrient inputs to the coastal ocean through submarine groundwater discharge: controls and potential impact. *J. Hydrol.* 295, 64–86. doi: 10.1016/j.jhydrol.2004.02.018

Stanev, E. V., Wolff, J.-O., Burchard, H., Bolding, K., and Flöser, G. (2003). On the circulation in the East Frisian Wadden Sea: numerical modeling and data analysis. *Ocean Dyn.* 53, 27–51. doi: 10.1007/s10236-002-0022-7

Staudigel, H., Yayanos, A., Chastain, R., Davies, G., Verdurmen, E. A. T., Schiffman, P., et al. (1998). Biologically mediated dissolution of volcanic glass in seawater. *Earth Planet. Sci. Lett.* 164, 233–244. doi: 10.1016/S0012-821X(98)00207-6

Street, J. H., Knee, K. L., Grossman, E. E., and Paytan, A. (2008). Submarine groundwater discharge and nutrient addition to the coastal zone and coral reefs of leeward Hawai'i. *Mar. Chem.* 109, 355–376. doi: 10.1016/J.MARCHEM.2007.08.009

Sugimoto, R., Kitagawa, K., Nishi, S., Honda, H., Yamada, M., Kobayashi, S., et al. (2017). Phytoplankton primary productivity around submarine groundwater discharge in nearshore coasts. *Mar. Ecol. Prog. Ser.* 563, 25–33. doi: 10.3354/meps11980

Swarzenski, P. W. (2007). U/Th series radionuclides as coastal groundwater tracers. *Chem. Rev.* 107, 663–674. doi: 10.1021/CR0503761

Tamborski, J., Beek, P., Rodellas, V., Monnin, C., Bergsma, E., Stieglitz, T., et al. (2019). Temporal variability of lagoon–sea water exchange and seawater circulation through a Mediterranean barrier beach. *Limnol. Oceanogr.* 1–22. doi: 10.1002/lno.11169

Tamborski, J., Bejannin, S., Garcia-Orellana, J., Souhaut, M., Charbonnier, C., Anschutz, P., et al. (2018). A comparison between water circulation and terrestrially-driven dissolved silica fluxes to the Mediterranean Sea traced using radium isotopes. *Geochim. Cosmochim. Acta* 238, 496–515. doi: 10.1016/j.gca.2018.07.022

Techer, I., Advocat, T., Lancelot, J., and Liotard, J. M. (2001). Dissolution kinetics of basaltic glasses: control by solution chemistry and protective effect of the alteration film. *Chem. Geol.* 176, 235–263. doi: 10.1016/S0009-2541(00)00400-9

Tréguer, P. J., and De La Rocha, C. L. (2013). The world ocean silica cycle. *Ann. Rev. Mar. Sci.* 5, 477–501. doi: 10.1146/annurev-marine-121211-172346

van Bemmelen, R. (1949). "Geological evolution of the physiographic units-Java," in *The Geology of Indonesia*, Vol. IA, ed. R. W. van Bemmelen, (The Hague: Government Printing Office), 554–559.

van Beusekom, J., and Diel-Christiansen, S. (2009). Global change and the biogeochemistry of the North Sea: the possible role of phytoplankton and phytoplankton grazing. *Int. J. Earth Sci.* 98, 269–280. doi: 10.1007/s00531-007-0233-8

Van Cappellen, P., Dixit, S., and van Beusekom, J. (2002). Biogenic silica dissolution in the oceans: reconciling experimental and field-based dissolution rates. *Global Biogeochem. Cycles* 16, 10–23. doi: 10.1029/2001GB001431

Van Cappellen, P., and Qiu, L. (1997). Biogenic silica dissolution in sediments of the Southern Ocean. I. Solubility. *Deep. Res. Part II Top. Stud. Oceanogr.* 44, 1109–1128. doi: 10.1016/S0967-0645(96)00113-0

Waltham, A., Smart, P., Friederich, H., and Eavis, A. (1983). The caves of Gunung Sewu, Java. *Cave Sci.* 10, 55–96.

Wang, G., Wang, Z., Zhai, W., Moore, W. S., Li, Q., Yan, X., et al. (2015). Net subterranean estuarine export fluxes of dissolved inorganic C, N, P, Si, and total alkalinity into the Jiulong River estuary, China. *Geochim. Cosmochim. Acta* 149, 103–114. doi: 10.1016/J.GCA.2014.11.001

Waska, H., Greskowiak, J., Ahrens, J., Beck, M., Ahmerkamp, S., and Böning, P. (2019). Spatial and temporal patterns of pore water chemistry in the inter-tidal zone of a high energy beach. *Front. Mar. Sci.* 6:154. doi: 10.3389/fmars.2019.00154

Webster, I. T., Hancock, G. J., and Murray, A. S. (1995). Modelling the effect of salinity on radium desorption from sediments. *Geochim. Cosmochim. Acta* 59, 2469–2476. doi: 10.1016/0016-7037(95)00141-7

Weinstein, Y., Yechieli, Y., Shalem, Y., Burnett, W. C., Swarzenski, P. W., and Herut, B. (2011). What is the role of fresh groundwater and recirculated seawater in conveying nutrients to the Coastal Ocean? *Environ. Sci. Technol.* 45, 5195–5200. doi: 10.1021/es104394r

Wiltshire, K. H., Boersma, M., Carstens, K., Kraberg, A. C., Peters, S., and Scharfe, M. (2015). Control of phytoplankton in a shelf sea: determination of the main drivers based on the helgoland roads time series. *J. Sea Res.* 105, 42–52. doi: 10.1016/j.seares.2015.06.022

Ye, Q., Liu, J., Du, J., and Zhang, J. (2016). Bacterial diversity in submarine groundwater along the coasts of the Yellow Sea. *Front. Microbiol.* 6:1519. doi: 10.3389/fmicb.2015.01519

Zektser, I. S., and Loaiciga, H. A. (1993). Groundwater fluxes in the global hydrologic cycle: past, present and future. *J. Hydrol.* 144, 405–427. doi: 10.1016/0022-1694(93)90182-9

Zhang, J., Zhang, G. S., and Liu, S. M. (2005). Dissolved silicate in coastal marine rainwaters: comparison between the yellow sea and the east china sea on the impact and potential link with primary production. *J. Geophys. Res.* 110:D16304. doi: 10.1029/2004JD005411

Conflict of Interest Statement: The authors declare that the research was conducted in the absence of any commercial or financial relationships that could be construed as a potential conflict of interest.